Improving the transparency of a rehabilitation robot by exploiting the cyclic behaviour of walking

W. van Dijk†, H. van der Kooij
Department of Biomechanical Engineering
Delft University of Technology
Delft, The Netherlands
w.vandijk@tudelft.nl

B. Koopman†, E.H.F. van Asseldonk, H. van der Kooij
Department of Biomechanical Engineering
MIRA, University of Twente
Enschede, The Netherlands
b.koopman@utwente.nl

† Equal contributors

***Abstract*— To promote active participation of neurological patients during robotic gait training, controllers, such as "assist as needed" or "cooperative control", are suggested. Apart from providing support, these controllers also require that the robot should be capable of resembling natural, unsupported, walking. This means that they should have a transparent mode, where the interaction forces between the human and the robot are minimal. Traditional feedback-control algorithms do not exploit the cyclic nature of walking to improve the transparency of the robot. The purpose of this study was to improve the transparent mode of robotic devices, by developing two controllers that use the rhythmic behavior of gait. Both controllers use adaptive frequency oscillators and kernel-based non-linear filters. Kernel-based non-linear filters can be used to estimate signals and their time derivatives, as a function of the gait phase. The first controller learns the motor angle, associated with a certain joint angle pattern, and acts as a feed-forward controller to improve the torque tracking (including the zero-torque mode). The second controller learns the state of the mechanical system and compensates for the dynamical effects (e.g. the acceleration of robot masses). Both controllers have been tested separately and in combination on a small subject population. Using the feed-forward controller resulted in an improved torque tracking of at least 52 percent at the hip joint, and 61 percent at the knee joint. When both controllers were active simultaneously, the interaction power between the robot and the human leg was reduced by at least 40 percent at the thigh, and 43 percent at the shank. These results indicate that: if a robotic task is cyclic, the torque tracking and transparency can be improved by exploiting the predictions of adaptive frequency oscillator and kernel-based nonlinear filters.**

***Keywords* — gait; rehabilitation robots; transparency; wearable robots; adaptive frequency oscillators; kernel-based non-linear filters**

I. INTRODUCTION

Robot-aided gait training is an emerging clinical tool for gait rehabilitation of neurological patients. These patients benefit form task oriented, high intensity, and repetitive training, to regain functional mobility [1-4]. Due to the repetitive behavior of gait training, rehabilitation robots are introduced. Robots can be used to provide more frequent, and more intensive training sessions, while reducing the workload of the therapist, compared to conventional forms of manual assisted (and body weight supported) gait training.

Despite the mentioned advantages of robotic-assisted gait training a large multicenter randomized clinical trial among stroke survivors suggested that the diversity of conventional gait training results in greater improvements in functional recovery than robotic-assisted gait training [5]. This emphasizes that robotic-assisted training needs to be further optimized in order to improve therapeutic outcome. Active patient participation is thought to be the key in achieving this improvement.

To encourage active participation, more and more robotic devices control the interaction forces with impedance or admittance control algorithms. Control strategies that promote active participation are often referred to as: "assist-as-needed" (AAN), "cooperative", "adaptive" or "interactive" controllers, and make the robot's behavior more flexible and adaptive to the patient's capabilities, progress and current participation. These types of controllers potentially increase the motivation of the patient since additional effort by the patient is reflected in their gait pattern. Additionally, depending on the impedance levels, small errors are still possible, which have been suggested to promote motor learning in mice [6, 7] as well as humans [8, 9].

A prerequisite of these control strategies is that the robot should have a transparent mode. When the patient does not require any support during specific subtasks or gait phases of walking, or when he increases his capabilities or effort, the robot should reflect normal unassisted walking. Due to the mass and inertia of the device, and/or imperfections in the controller for the transparent mode, unassisted walking is often different from free walking [10, 11].

In a perfect transparent mode there are no interaction forces between the subject and the robot. In our gait rehabilitation robot, Lopes (Fig. 1), the transparent mode consists of a zero-torque mode, where torques at the robot joints are controlled to zero. This does however not result in a perfect transparent mode and causes small gait alterations [11]. These

Manuscript received January 31, 2012. This work was supported by the EU within the EVRYON Collaborative Project (Evolving Morphologies for Human-Robot Symbiotic Interaction, Project FP7-ICT-2007-3-231451).

978-1-4673-6024-1/13/$31.00 ©2013 IEEE

imperfections are partly due to sensor noise and friction in the actuation that limit the gains of the PI-controller, resulting in torque tracking errors. Additionally, the forces that occur due to joint friction, gravity, and inertias of the moving segments of the Lopes, are not compensated for in the current implementation. It is possible to compensate for these forces by an additional controller [12].

As mentioned before, Lopes, like many other rehabilitation robots, is specifically designed to assist a cyclic task, in this case walking. Robotic performance of cyclic tasks can be improved by repetitive control or adaptive control [13]. The latter has been implemented on the Lokomat rehabilitation robot in order to increase the compliance and transparency of this robot. One of the proposed controllers for this robot minimizes human-robot interaction forces by on-line optimization of a limited number of gait characteristics (angle offset, amplitude, and cycle time) of the reference angle trajectory used by their impedance controller [14]. Thus, the robot motion gets entrained with the desired human motion. In this paper we present a more general framework for improved torque control, and improved transparent control. Therefore we developed two new controllers. Both controllers use a framework of adaptive frequency oscillators and kernel-based non-linear filters to learn a control signal [15, 16].

The first controller is intended to improve the limited torque tracking of the currently implemented PI-controller. As suggested by Kuo the control of rhythmic movements can be improved by combining feedback and feed-forward control [17]. In general, feed-forward control requires a precise model of the dynamic system. To establish this model, precise system identification is required which is, for many applications, a limitation to implement feed-forward control strategies. In this special case however we can use the information from previous cycles to learn the feed-forward signal in a model-free manner, and gradually learn the feed-forward signal over multiple cycles.

The second controller compensates for the passive dynamics of the system that exist between the actuator and the user. This includes: gravitational, inertial and frictional forces. Forces that emerge from these effects are not sensed, and therefore not compensated, in the zero-torque mode. Compensation of these forces is achieved by the implementation of an inverse model, which in this case is an inverse dynamical model of the Lopes exoskeleton legs. The forces calculated by the inverse model are opposite to the existing forces. Application of the calculated forces should, theoretically, cancel out the interaction forces between the robot and the human.

Both controllers are tested separately and in combination on a small group of healthy test subjects (N=4). To evaluate the performance of both control strategies the applied torques, the human-robot interaction forces, as well as the joint angles, are tracked. Here the suggested control strategies are specifically applied and tuned for the Lopes gait rehabilitation robot, but both approaches can be applied to other applications as well, as long as it concerns cyclic movement.

Fig. 1: The Lopes is a bilateral exoskeleton with eight degrees of freedom. The actuators are detached from the exoskeleton and connected to the joints via Bowden cables and springs. The robot is impedance controlled via series elastic actuation.

II. Experimental Setup and Methodology

A. *Subjects*

Four healthy subjects (4 males, age: 28 ± 2 years, height: 1.80 ± 0.03 m, weight: 74.5 ± 11.2 kg) participated in this experiment. All subjects gave written informed consent prior to participation.

B. *Experimental apparatus and recordings*

To test both controllers the Lopes was used. The Lopes (Fig. 1) is a treadmill-based lower-limb exoskeleton type robotic gait trainer. The Lopes is impedance-controlled and has eight actuated degrees of freedom (DoF) (flexion/extension at the hip and knee, hip abduction/adduction and horizontal pelvis translations). The robot was initially designed to provide supported treadmill training for stroke patients. Torque control was achieved by Bowden-cable-driven, PI-controlled, series-elastic actuators [18]. The actuators themselves were controlled

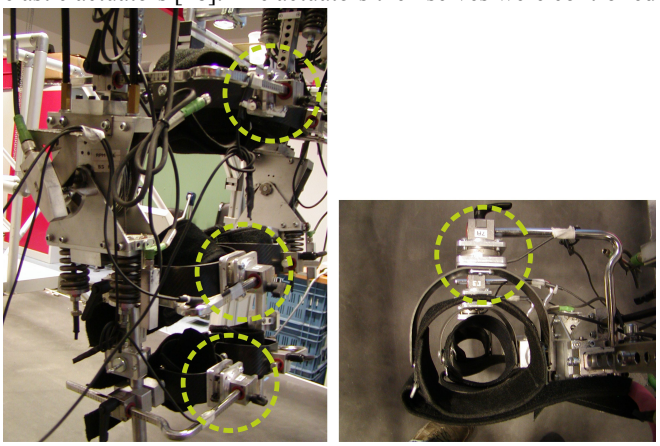

Fig. 2**:** Six DoF force sensors (encircled). The force sensors are, via carbon shells and Velcro straps, attached to the human at one side and to the robot on the other side. Interaction forces are measured at the thigh (1 connection) and the shank (2 connections, high, and low)

with an inner velocity feedback loop [19]. Every DoF of the Lopes was fitted with potentiometers that record the kinematics, and potentiometers on the springs of the SEA that record the applied torque. Matlab xPC (Mathworks, Natick, Mass., USA) was used to control the applied torques by the exoskeleton joints at 1000 Hz. The performance of the used PI controller is described in [19].

Additionally the interface between the subject's legs and the exoskeleton legs was sensorized using three (six DoF) force sensors (ATI-Mini45-SI-580-20, ATI Industrial Automation, Apex, N.C., USA, Fig. 2). The cuffs (Hocoma, Volketswil, Switzerland) used in the Lopes were made of a rigid carbon fiber shell with Velcro straps and secure the subject's legs to the robot. One cuff connected to the upper leg and two cuffs connected to the lower leg of the subject. Only the interface of the right leg was fitted with force sensors. The analog signals coming from the force sensors were sampled at 1000 Hz using a data acquisition system (NI usb-6259, National Instruments, Austin, Texas, USA) and sent to the computer, where the data was stored for further processing. For clarity, the force sensors were only used to quantify the human-robot interaction forces, which were used as a measure for the transparency, and not as an input to the controller.

C. Controller design

For the controllers that are presented in the next sections, an estimate of the position signals and their first and second order derivatives are required. To learn these signals the approach as suggested by [15] was used, which uses adaptive frequency oscillators in combination with kernel-based non-linear filters.

1) Adaptive frequency oscillator

Positions and their time derivatives can be expressed as a function of the gait phase. To acquire the gait phase, an adaptive frequency oscillator [20] matches a sinusoidal signal to an input signal. The phase of the sinusoidal signal was used as the gait phase (ϕ) that runs from 0 to 2π. In our application the right and left hip angle were used as input signals, since they show a sinusoidal like profile. The right and left hip angle (θ_{right} and θ_{left}) were estimated with the following sinusoidal functions:

$$\hat{\theta}_{right}(t) = k + a \cdot \sin\left(\varphi(t)\right), \quad \hat{\theta}_{left}(t) = k + a \cdot \sin\left(\varphi(t) + \pi\right) \tag{0.1}$$

Of which k, a, and ϕ are the offset, amplitude and the phase of the signal respectively and t is the time in seconds, the circumflex ($\hat{}$) denotes a signal estimate by the adaptive frequency oscillator. The left and right hip motions were assumed identical, with only a phase shift of π. The signal parameters were continuously updated using two error functions (e).

$$\begin{aligned} e_{right}(t) &= \theta_{right}(t) - \hat{\theta}_{right}(t) \\ e_{left}(t) &= \theta_{left}(t) - \hat{\theta}_{left}(t) \end{aligned} \tag{0.2}$$

The following differential equations are governing the update process of the sinusoidal signal parameters:

$$\begin{aligned} \dot{\varphi}(t) &= \omega + \varepsilon e_{right}(t)\cos\left(\varphi(t)\right) + \varepsilon e_{left}(t)\cos\left(\varphi(t) + \pi\right) \\ \dot{\omega}(t) &= \varepsilon e_{right}(t)\cos\left(\varphi(t)\right) + \varepsilon e_{left}(t)\cos\left(\varphi(t) + \pi\right) \\ \dot{a}(t) &= \eta\left(e_{right}(t)\sin\left(\varphi(t)\right) + e_{left}(t)\sin\left(\varphi(t) + \pi\right)\right) \\ \dot{k}(t) &= \eta\left(e_{right}(t) + e_{left}(t)\right) \end{aligned} \tag{0.3}$$

The parameter ω [rad s^{-1}] estimated the frequency of the stride. Constants η and ε were used to regulate the learning rate of the signal. Pre-trials showed that with a η and ε of respectively 0.4 and 2 the adaptive frequency oscillator was synchronized within approximately ten steps.

2) Kernel-based non-linear filters

Subsequently, the position signals and their first and second order time-derivatives were estimated. The obtained gait phase of the adaptive frequency oscillator was used to learn the joint angles and the motor angles as a function of the phase. We used kernel-based non-linear filters as presented by [15] to learn the signal as a sum of n Gaussian functions ($\psi(t)$):

$$\psi_i(t) = \exp\left(h\left(\cos\left(\varphi(t) - c_i\right) - 1\right)\right) \quad i = 1..n \tag{0.4}$$

with

$$c_i = \frac{2\pi i}{n} \tag{0.5}$$

where h is a parameter that determines the width of the Gaussian function. Pre-trials showed that with n is 20 and an h of 15 the learned signal matched the angular pattern of the hip and knee well. The learned signal ($\tilde{\theta}(t)$) was estimated on time (t) with:

$$\tilde{\theta}(t) = \frac{\sum_{i=1}^{n} w_i(t)\psi_i(t)}{\sum_{i=1}^{n} \psi_i(t)} \tag{0.6}$$

The tilde ($\tilde{}$) denotes the signal estimated by the non-linear filter. The weights (w) were adapted according to:

$$\dot{w}(t) = P\psi\left(\theta(t) - \tilde{\theta}(t)\right) \tag{0.7}$$

Where P had a value of 3 and is the learning gain, determining how fast the filter adapted its prediction. When the non-linear filter had learned the characteristics of the signal the filter can be locked by setting $\dot{w}$ to zero. A nice feature of this filter is that analytical derivatives of the signal estimate can be obtained, which provided the velocity and acceleration estimate that was needed for the improved torque tracking and the improved transparency. The frequency and weights were only changing relatively slow and therefore assumed constant:

$$\dot{\varphi}(t) = \omega \text{ and } \dot{w}(t) = 0 \tag{0.8}$$

Additionally it was assumed that:

$$\frac{d}{dt}\left(\sum_{i=1}^{n} \psi_i(t)\right) = 0 \tag{0.9}$$

This is approximately true if a sufficient large number of kernels is chosen. The first time derivative is:

TABLE 1: DYNAMIC PROPERTIES LOPES

	Thigh	**Shank**
Mass [kg]	5.9	4.2
Inertia [kg m^2]	0.079	0.044
Length [m]	0.44	--
Centre of mass [m]	0.2	0.2
Damping [Nm^{2}s^{-1}]	0.98	0.54
Strap position [m]	0.32	0.15 and 0.29

Dynamical properties of the Lopes rehabilitation robot. Distances are measured from the proximal joint of the segment.

$$\tilde{\dot{\theta}} = \frac{\sum_{i=1}^{n} w_i(t)\dot{\psi}_i(t)}{\sum_{i=1}^{n} \psi_i(t)} \tag{0.10}$$

with

$$\dot{\psi}_i(t) = -\psi_i(t)h\omega\sin\left(\varphi(t) - c_i\right) \tag{0.10}$$

And the second time derivative is:

$$\tilde{\ddot{\theta}} = \frac{\sum_{i=1}^{n} w_i(t)\ddot{\psi}_i(t)}{\sum_{i=1}^{n} \psi_i(t)} \tag{0.11}$$

with

$$\begin{aligned}\ddot{\psi}_i(t) = &-\dot{\psi}_i(t)h\omega\sin\left(\varphi(t) - c_i\right) \\ &\cdot\psi_i(t)h\omega^2\cos\left(\varphi(t) - c_i\right)\end{aligned} \tag{0.12}$$

3) Feed-forward velocity learning controller

In the Lopes the series-elastic actuators were originally PI-controlled. Within this setup sensor noise and friction in the actuation limited the maximal feedback gains that can be used, resulting in tracking errors. The cyclic behavior of walking provides the possibility to estimate a feed-forward signal. The feed-forward signal was obtained with a non-linear filter. This filter learned the motor angles, (θ_{motor} , from the motor encoder) as a function of the phase, according to eq. 0.6. The analytical derivative (eq. 0.10) of the estimated signal ($\tilde{\dot{\theta}}_{motor}$) was used as the feed-forward signal in the Lopes torque control loop (which is velocity controlled). This signal was added to the motor-velocity command ($\dot{\theta}_{PI}$) from the PI-controller and was sent to the actuators. Fig. 3 shows this control strategy.

4) Dynamics compensation controller

In the original transparent mode the joint torques were regulated to zero (zero-torque mode). Even if this control works perfectly this does not mean that the human, who walks in the Lopes, does not experience any interaction forces (F). Friction, gravity and inertia will still result in reaction forces that are felt via the connections with the Lopes. An inverse dynamics module can be used to calculate the torques (τ_{ID}) required to cancel these interaction forces.

The inverse dynamics module described two planar double pendulums. Each double pendulum represented one leg of the Lopes in the sagittal plane, consisting of an upper and lower leg segment. Each segment of the pendulums had a mass (located at a certain distance from the proximal joint) and inertia. Additionally, each joint had rotational damping, which represented friction in each joint. The parameters corresponding to the different Lopes segments were estimated using multi-input-multi-output (MIMO) system identification [21]. Table 1 provides an overview of the system parameters. The input of the inverse model consisted of the hip and knee angle, angular velocity, and angular acceleration. The Lopes was not fitted with accelerometers that measure the required signals directly. Therefore, the joint angles and their first and second order derivatives were also obtained with the non-linear filter. Fig. 3 shows this control strategy.

D. Experimental protocol

Before the subject was positioned in the Lopes, different anthropometric measurements were taken to adjust the exoskeleton segment lengths. Additionally, the positions of the

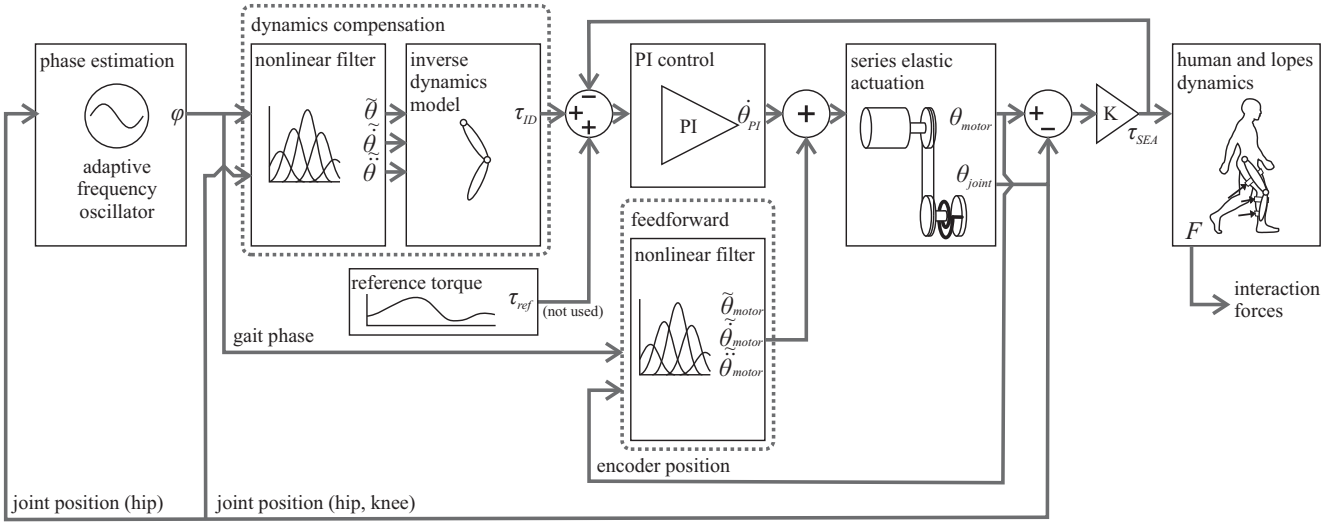

Fig. 3: A schematic overview of the implemented controllers on the Lopes rehabilitation robot. The dynamics compensation module and the velocity learning module can be switched off so their output becomes zero. In the experiments described here the transparent mode was evaluated so the reference torque is set to zero.

cuffs were adjusted to align the subject's knee and hip axis with the exoskeleton joints. Next, the subject was positioned into the Lopes and the trunk, thigh, and upper- and lower shank were strapped to the exoskeleton (Fig. 2).

After a 5 minute familiarization period, to get used to walking in the Lopes, each subject performed two trials. The trials were performed at a slow walking (0.5 ms^{-1}) and fast walking speed (1.0 ms^{-1}). First the subjects walked for ninety seconds in the device using only the PI-controller (the conventional zero-torque mode). During this period the subject's cadence was recorded. The interaction forces scale with the cadence and the walking speed. At higher walking speeds the exoskeleton legs are accelerated and decelerated more, resulting in higher interaction forces. To cancel this effect out, the different controllers were tested at a fixed treadmill speed and a fixed cadence. The fixed cadence was achieved by asking the subjects to synchronize their walking tempo with a metronome that was set to the average of the subjects' pre-recorded cadence. This first condition (90 seconds of PI-controller) was also used to learn the signals that were required for the dynamics compensation. After 90 seconds the non-linear filters, that learn the hip and the knee angle (and their derivatives), were locked. Subsequently the different controllers were tested. The non-linear filter for the feed-forward controller was not locked. The different walking conditions and their duration are listed in Table 2. All conditions (at one speed) were evaluated directly after each other at the same cadence, without interruptions. In the second trial this protocol was repeated for the fast walking speed.

E. Data analysis

All signal processing was done with custom-written software in Matlab (Natick, Mass., USA). The measured forces from the three force sensors were resampled at 100 Hz and synchronized with the potentiometer data from the Lopes.

Of all the recorded conditions only the last 60 seconds were used for data processing. Performance of the controllers was calculated based on the root mean square (RMS) of different signals. The evaluated signals were: 1) the torque tracking error, 2) the interaction force in the sagittal plane (perpendicular to the exoskeleton legs), and 3) the interaction power. The interaction power was calculated by taking the product of the moment of the interaction forces around their proximal joint and the velocity of their proximal joint. Results for the upper and lower shank force were summed. The power provides a measure for the flow of energy between robot and human, that is: it shows how much the robot is supporting, or resisting, the movement of the human.

Average steps were calculated by splitting the data into individual strides, based on the heel-contact event. Next, the

TABLE 2: CONDITIONS

Condition	Duration for each speed (s)
PI	90
PI + velocity learning	90
PI + dynamics compensation	90
PI + velocity learning + dynamics compensation	90

TABLE 3: REDUCTIONS IN RMS TORQUE ERROR

	Dynamics compensation off		Dynamics compensation on	
	Slow	***Fast***	***Slow***	***Fast***
Hip	52% *(49%-56%)*	59% *(51%-60%)*	56% *(53%-64%)*	58% *(51%-62%)*
Knee	61% *(55%-68%)*	64% *(55%-70%)*	65% *(63%-67%)*	62% *(61%-63%)*

Reductions in RMS of the difference between desired and recorded torque (tracking error), averaged over the subjects. All reductions were significant with $p < 0.01$ (paired t-test). The values between brackets show the range of the data over the different subjects.

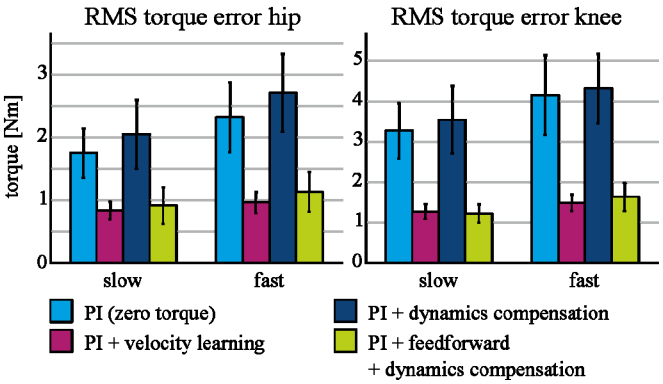

Fig. 4: RMS of the tracking error at the hip (left) and knee (right). The bars are the results, averaged over the subjects. The error bars denote the standard deviations.

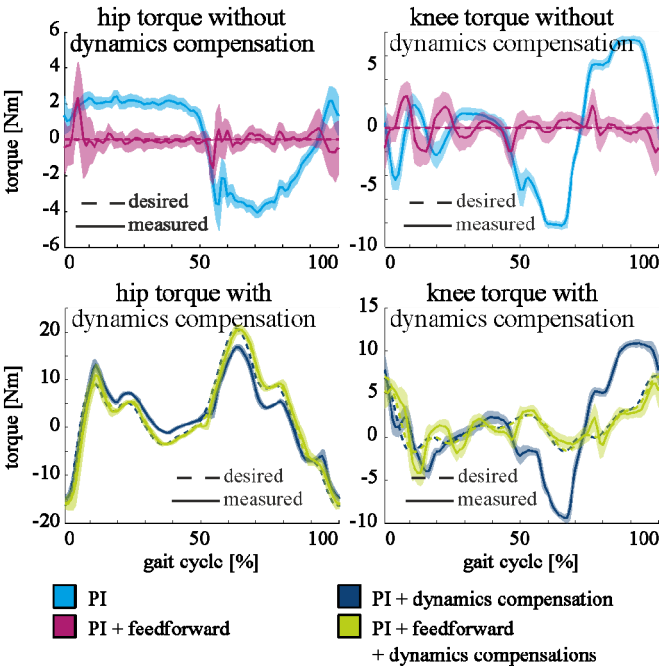

Fig. 5: Top: difference between the desired and the measured torque without dynamics compensation (zero-torque mode) Bottom: difference between both signals with dynamics compensation. The figure shows the results for a typical subject. All signals are presented as a function of the gait cycle, starting at heel strike. Left: results for the hip. Right: results for the knee.

different data blocks were normalized as a percentage of the gait cycle and averaged. Paired t-tests were performed to test for significant differences between the conditions. The level of significance was defined at p=0.05.

III. Results

A. Torque tracking

The torque tracking was improved by the feed-forward controller. The RMS of the torque tracking error (RMSE) significantly reduced (Table 3, Fig. 4). Reductions in tracking error were similar in the zero-torque mode and with the dynamics compensation switched on (Table 3). The small standard deviation indicates that all subjects showed similar reductions. In general the knee joint had the largest reduction in RMSE. No clear effect of the walking speed on the tracking error was observed. A typical example of the tracking error as a function of the gait cycle, with and without the dynamics compensation, is shown in Fig. 5.

B. Interaction forces

For the thigh, the interaction forces were reduced when the feed-forward controller was switched on, compared to the zero-torque mode (Fig. 6). The dynamics compensation also resulted in a reduction in thigh interaction forces compared to the zero-torque mode. An additional decrease was observed when the feed-forward controller was switched on in combination with the dynamics compensation, leading to a total reduction of interaction forces of 39% (p = 0.001) for slow walking and 35% (p = 0.009) for fast walking. Walking at higher speed showed the same trends. In general: a higher walking speed resulted in higher interaction forces between subjects and robot.

For the interaction forces on the lower leg (shank high and shank low) the dynamics compensation did not result in a reduction of the forces, compared to the zero-torque mode (Fig. 6). In fact: the interaction forces increased slightly. In contrast, the feed-forward controller did reduce the interaction forces. When it was switched on in the zero-torque mode, as well as in combination with the dynamics compensation, it resulted in reduced interaction forces.

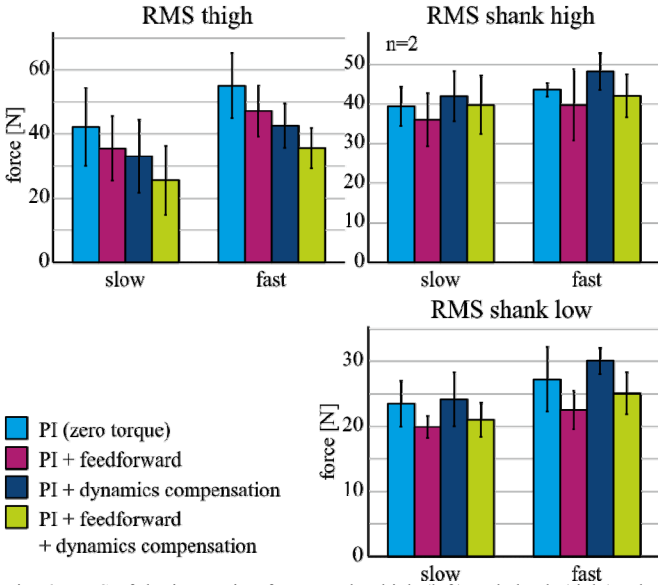

Fig. 6: RMS of the interaction forces at the thigh (left) and shank (right). The bars are the results, averaged over the subjects. The error bars denote the standard deviations.

C. Interaction power

The interaction power (Fig. 7) showed the same trends as observed in the interaction forces (Fig. 6). At the thigh the dynamics compensation resulted in a reduction in power compared to the zero-torque mode. An additional decrease was observed when the feed-forward controller was switched on (Fig. 7). Combining both controllers led to a total reduction of interaction power of 40.9% (p = 0.002) for slow walking and 40.2% (p = 0.007) for fast walking. Looking solely at the effect of walking speed, walking at higher speeds resulted in larger powers.

For the lower leg the dynamics compensation alone did not result in a clear reduction of the interaction power, compared to the zero-torque mode (Fig. 7), but the feed-forward controller did reduce the interaction power. In contrast to the interaction

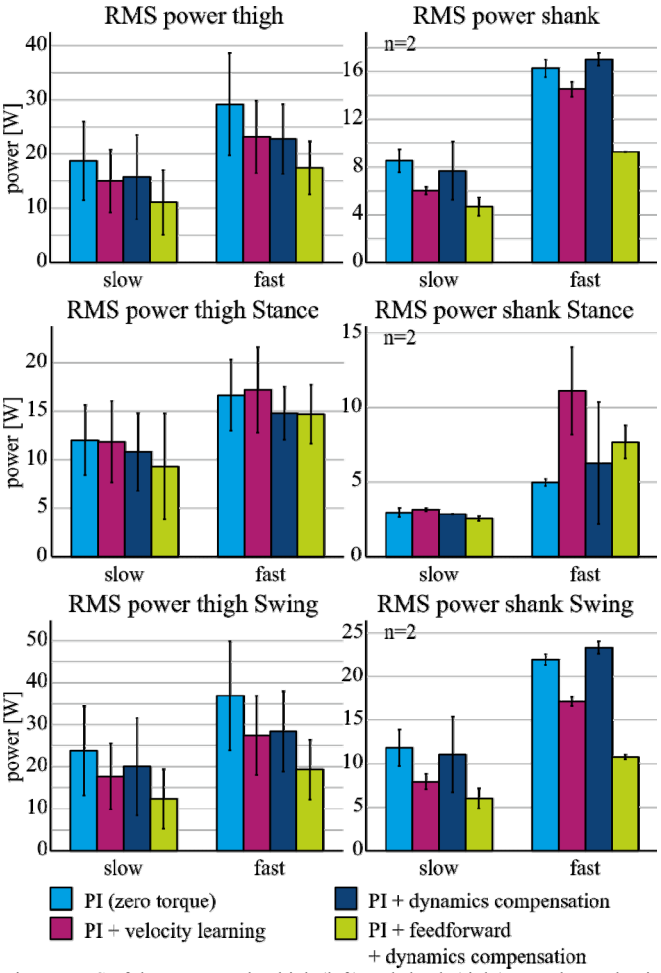

Fig. 7: RMS of the power at the thigh (left) and shank (right) over the total gait cycle (top) and divided in stance (middle) and swing phase (bottom). The bars are the results, averaged over the subjects. The error bars denote the standard deviations.

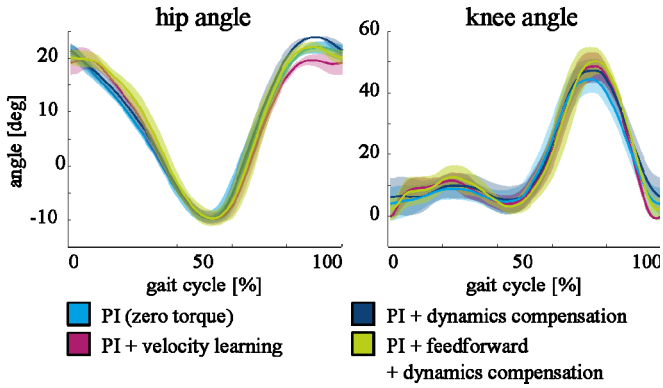

Fig. 8: Gait kinematics averaged over the subjects (flexion is positive), and presented as a function of the stride, starting at heel strike. Shaded areas show the standard deviations between the subjects.

force (Fig. 6), combining both controllers resulted in a large reduction in the power at the shank (slow walking 45.3%, fast walking 43.2%).

Figure 7 also shows that the dynamics compensation resulted in a larger reduction in interaction power during the swing phase than during the stance phase.

D. *Kinematics*

The recorded joint angles are compared for the different controllers in Fig. 8. Gait kinematics show only subtle differences. The most prominent difference is the increase in knee flexion angle. If the feed-forward controller and the dynamics compensation are on simultaneously the maximal knee ankle is 5.8 degrees larger than the condition where both controllers are off ($p = 0.003$).

IV. Discussion

The purpose of this study was to investigate how the cyclic nature of many rehabilitation tasks could be exploited to improve the control and transparency of rehabilitation robots. The results for the two tested controllers are discussed below.

A. *Feed-forward velocity learning controller*

The RMS of the torque tracking error showed a large improvement. Still, our approach can only filter out errors that are cyclic, with the same cycle time as the gait cycle (Fig. 5). Errors that are not a function of the gait phase cannot be captured by the non-linear filter. The remaining error in the torque tracking is partly due to tracking errors that are not cyclic. However, in our study the cyclic effects were dominant and the RMSE could be reduced by more than half.

B. *Dynamics compensation*

The effect of the dynamics compensation was measured by the interaction power. When the dynamics compensation was switched on the interaction power reduced, especially for the thigh (Fig. 7). Our results also indicate that the effect of the dynamics compensation controller is larger if the feed-forward velocity controller is active in parallel, which clearly improved the torque tracking (Fig. 4). This indicates that a good torque tracking is a prerequisite for the dynamics compensation controller to work, especially since the desired torques are relatively small (Fig. 5).

In general the dynamics compensation controller showed a larger reduction in interaction power during the swing phase than during the stance phase (Fig. 7). This might be due to larger joint accelerations during the swing phase, than during the stance phase. Larger accelerations correspond to larger forces that can be compensated for with this controller. Indeed, Fig. 7 shows higher interaction powers during the swing phase compared to the stance phase.

An additional possible explanation is that the interaction forces, during the stance phase, have a source that cannot be compensated for by either one of the controllers. As a safety measure the Lopes has a mechanical end-stop at the knee joint to prevent hyperextension. At initial heel contact, at the beginning of the stance phase, the subject is likely to hit that end-stop and the Lopes cannot reduce the interaction forces by further extending.

Some of the remaining interaction forces might emerge from a misalignment between the human and the robot leg. This cannot be compensated for by the controllers, but can only be solved with a more ergonomic design.

Evaluation of the kinematics showed an increase in maximum knee angle during the swing (Fig. 8). This suggest that, in our specific case, the previous observed reduction in knee flexion [11] (in de zero-torque mode) was compensated for by our controllers. This might indicate that the subjects have a more natural gait when the controllers are switched on. Up to this point we did not investigate the changes in human performance in terms of the kinematic resemblance of natural walking, energy expenditure or muscle activation. This will be part of further research.

V. Conclusion

If a robotic task is cyclic, the performance of this task can be improved by exploiting the predictions of adaptive frequency oscillator and kernel-based nonlinear filters. These filters predict signals for the upcoming steps. This prediction can be used to compose a feed-forward signal to increase robotic control accuracy. We showed that for our rehabilitation robot we improved the torque tracking and reduced the interaction forces between the robot and the human, and thereby improved the transparency of our robot. Still we need to evaluate how the controllers react to sudden gait changes and irregular gait patterns.

VI. References

[1] G. Kwakkel, R. van Peppen, R. C. Wagenaar, S. Wood Dauphinee, C. Richards, A. Ashburn, K. Miller, N. Lincoln, C. Partridge, I. Wellwood, and P. Langhorne, "Effects of augmented exercise therapy time after stroke: a meta-analysis," *Stroke,* vol. 35, pp. 2529-39, Nov 2004.

[2] G. Kwakkel, R. C. Wagenaar, T. W. Koelman, G. J. Lankhorst, and J. C. Koetsier, "Effects of intensity of

rehabilitation after stroke. A research synthesis," *Stroke,* vol. 28, pp. 1550-6, Aug 1997.

[3] R. Teasell, J. Bitensky, K. Salter, and N. A. Bayona, "The role of timing and intensity of rehabilitation therapies," *Top Stroke Rehabil,* vol. 12, pp. 46-57, Summer 2005.

[4] N. A. Bayona, J. Bitensky, K. Salter, and R. Teasell, "The role of task-specific training in rehabilitation therapies," *Top Stroke Rehabil,* vol. 12, pp. 58-65, Summer 2005.

[5] J. Hidler, D. Nichols, M. Pelliccio, K. Brady, D. D. Campbell, J. H. Kahn, and T. G. Hornby, "Multicenter randomized clinical trial evaluating the effectiveness of the Lokomat in subacute stroke," *Neurorehabil Neural Repair,* vol. 23, pp. 5-13, Jan 2009.

[6] L. L. Cai, A. J. Fong, C. K. Otoshi, Y. Q. Liang, J. G. Cham, H. Zhong, R. R. Roy, V. R. Edgerton, and J. W. Burdick, "Effects of consistency vs. variability in robotically controlled training of stepping in adult spinal mice.," in *9th International Conference on Rehabilitation Robotics*, Chicago, IL, USA, 2005.

[7] M. D. Ziegler, H. Zhong, R. R. Roy, and V. R. Edgerton, "Why variability facilitates spinal learning," *J Neurosci,* vol. 30, pp. 10720-6, Aug 11 2010.

[8] S. Jezernik, R. Scharer, G. Colombo, and M. Morari, "Adaptive robotic rehabilitation of locomotion: a clinical study in spinally injured individuals," *Spinal Cord,* vol. 41, pp. 657-66, Dec 2003.

[9] J. L. Emken and D. J. Reinkensmeyer, "Robot-enhanced motor learning: accelerating internal model formation during locomotion by transient dynamic amplification," *IEEE Trans Neural Syst Rehabil Eng,* vol. 13, pp. 33-9, Mar 2005.

[10] J. L. Emken, J. H. Wynne, S. J. Harkema, and D. J. Reinkensmeyer, "A robotic device for manipulating human stepping," *IEEE Transactions on Robotics,* vol. 22, p. 185, 2006.

[11] E. H. van Asseldonk, J. F. Veneman, R. Ekkelenkamp, J. H. Buurke, F. C. van der Helm, and H. van der Kooij, "The Effects on Kinematics and Muscle Activity of Walking in a Robotic Gait Trainer During Zero-Force Control," *IEEE Trans Neural Syst Rehabil Eng,* vol. 16, pp. 360-370, Aug 2008.

[12] H. Vallery, A. Duschau-Wicke, and R. Riener, "Generalized elasticities improve patient-cooperative control of rehabilitation robots," in *Rehabilitation Robotics, 2009. ICORR 2009. IEEE International Conference on*, 2009, pp. 535-541.

[13] Y. Wang, F. Gao, and F. J. Doyle Iii, "Survey on iterative learning control, repetitive control, and run-to-run control," *Journal of Process Control,* vol. 19, pp. 1589-1600, 2009.

[14] R. Riener, L. Lunenburger, S. Jezernik, M. Anderschitz, G. Colombo, and V. Dietz, "Patient-cooperative strategies for robot-aided treadmill training: first experimental results," *Neural Systems and Rehabilitation Engineering, IEEE Transactions on,* vol. 13, pp. 380-394, 2005.

[15] A. Gams, A. J. Ijspeert, S. Schaal, and J. Lenarčič, "On-line learning and modulation of periodic movements with nonlinear dynamical systems," *Autonomous robots,* vol. 27, pp. 3-23, 2009.

[16] R. Ronsse, T. Lenzi, N. Vitiello, B. Koopman, E. Van Asseldonk, S. M. M. De Rossi, J. Van Den Kieboom, H. Van Der Kooij, M. C. Carrozza, and A. J. Ijspeert, "Oscillator-based assistance of cyclical movements: model-based and model-free approaches," *Medical and Biological Engineering and Computing,* pp. 1-13, 2011.

[17] A. D. Kuo, "The relative roles of feedforward and feedback in the control of rhythmic movements," *MOTOR CONTROL-CHAMPAIGN-,* vol. 6, pp. 129-145, 2002.

[18] J. F. Veneman, R. Kruidhof, E. E. G. Hekman, R. Ekkelenkamp, E. H. F. Van Asseldonk, and H. Van der Kooij, "Design and Evaluation of the LOPES Exoskeleton Robot for Interactive Gait Rehabilitation," *IEEE Trans Neural Syst Rehabil Eng,* vol. 15, pp. 379-386, Sep 2007.

[19] H. Vallery, R. Ekkelenkamp, H. van der Kooij, and M. Buss, "Passive and Accurate Torque Control of Series Elastic Actuators," in *IEEE International Conference on Intelligent Robots and Systems*, San Diego, USA, 2007, pp. 3534-3538.

[20] L. Righetti, J. Buchli, and A. J. Ijspeert, "Dynamic Hebbian learning in adaptive frequency oscillators," *Physica D: Nonlinear Phenomena,* vol. 216, pp. 269-281, 2006.

[21] B. Koopman, E. van Asseldonk, and H. van der Kooij, "In vivo measurement of human knee and hip dynamics using MIMO system identification," in *EMBC*, Buenos Aires 2010, pp. 3426-3429.